



## **Buckling strength sensitivity for thin-walled tubes with complex imperfections**

Ziqi Tang<sup>1</sup>, Dehui Lin<sup>2</sup>, Benjamin W. Schafer<sup>3</sup>, Andrew T. Myers<sup>4</sup>, Michael D. Shields<sup>5</sup>

### **Abstract**

Thin-walled tubes are widely used for civil infrastructure, such as wind turbine support towers. These tubes have inevitable defects arising from manufacturing. Like all shells, these imperfections can trigger a variety of collapse mechanisms and lead to highly variable strength. Classically this is understood as deriving from a complex interplay between the imperfection shape and the many nearly coincident buckling modes that exist in such shells. The conventional numerical approach to assess the influence of these imperfections is to include structural defects using the primary buckling modes (e.g., modes 1-3) in a geometric and material nonlinear shell finite element analysis on the imperfect structure, i.e., a GMNIA solution. Measured imperfections typically do not take the form of the primary buckling modes. Instead, imperfections have more complex shapes that can be understood as combinations of several higher-order modes that potentially induce failures. However, it remains unclear which combinations of higher modes result in significant reductions in buckling strength, so there is little guidance as to which modes should be included in imperfection models. Assessing the sensitivity of buckling strength to imperfections from mode combinations is, therefore, critical to understanding which higher modes should be included in imperfection models. In this study, we impose imperfections as combinations of the first one hundred axial and bending buckling modes, then perform GMNIA collapse simulations under uniform bending with different magnitudes to assess the strength sensitivity. In addition, we also geometrically categorized the mode shapes to assess sensitivity according to a characteristic length-scale (wavelength) of each mode and observe the specific imperfection features that cause large drops in strength. The intent of the work is to build imperfection characterizations that are optimally informed by structural features that drive strength.

### **1. Introduction**

Thin-walled steel tubes, a component widely used in civil infrastructures, have a high strength-to-weight ratio and the ability to withstand large loads. However, the strength of thin-walled tubes is acutely sensitive to the magnitude and distribution of geometric imperfections (Seide et al. 1965, Calladine 1995), which are, in turn, dependent on the manufacturing process. This sensitivity

---

<sup>1</sup> Graduate Research Assistant, Johns Hopkins University, <ztang20@jhu.edu>

<sup>2</sup> Ph.D. candidate, Northeastern University, <lin.deh@northeastern.edu>

<sup>3</sup> Professor, Johns Hopkins University, <schafer@jhu.edu>

<sup>4</sup> Associate Professor, Northeastern University, <atm@northeastern.edu>

<sup>5</sup> Associate Professor, Johns Hopkins University, <michael.shields@jhu.edu>

manifests itself in two important ways: strengths that decrease with increasing diameter-to-thickness ratio ( $D/t$ ) and large scatter in measurements of strength. For wind turbine support towers, the external loads induce primary bending at the base of the towers, and thus the imperfection sensitivity of these thin-walled steel tubes in flexure is of major interest. Conventional methods for evaluating the influence of geometric imperfections on the bending strength of thin-walled tubes often rely on the eigenmode-affine pattern (Eurocode EN 1993-1-6: 2007), in which certain buckling modes obtained from an eigen-buckling analysis are used as "equivalent" imperfections. This approach assumes that the most important sensitivities in the shells are associated with the selected buckling modes, and thus can be used to predict the bending capacity. This method typically includes imperfections from the first few buckling modes (e.g., modes 1-3) in a geometric and material nonlinear shell finite element analysis of the imperfect tube (a.k.a, GMNIA). Eigenmode-affine imperfections typically do not accurately capture the characteristics of measured imperfections from manufacturing. Observed imperfections often have more complex shapes, which can be understood as requiring higher-order modes or combinations of several modes. It remains unclear which mode combinations best balance accurately re-creating measured imperfections and realistically assessing the most significant reductions in strength, and there is little guidance to the selection of modes. Assessing the sensitivity of strength to imperfections from mode combinations is, therefore, useful in understanding which higher modes should be included in imperfection models.

### *1.1 Thin-walled structural tubes – Wind turbine tower applications*

Thin-walled tubes are cylindrical structures with a large outer diameter and small wall thickness. They are commonly used in various engineering applications, such as in the construction of aircraft, pipelines, and civil engineering structures. One of their primary, and rapidly growing, uses is for wind turbine tower construction. Wind turbine towers are very tall and slender structures that support the weight of the wind turbine and its rotor blades, as well as the loads imposed on the turbine by the wind and other external forces. These towers are tall, often exceeding  $h = 150$  meters in height and have very thin walls with diameter-to-thickness ratios ( $D/t$ ) between 100 and 350 (Ding et al. 2021). Moreover, there is increasing motivation to build taller towers that reach into higher, more steady winds with higher  $D/t$ , therefore requiring less steel for construction. However, as both  $h$  and  $D/t$  grow larger, these structural tubes become increasingly sensitive to small geometric defects.

The design process of these structures involves a detailed analysis of the critical loads acting on the tower to predict its behavior and ensure structural integrity. Large-scale structural tubes for wind turbine tower applications are subject to complex, stochastic time-varying loads that combine bending from wind-induced overturning forces and torsion from wind action on the turbine blades (see Fig. 1). In comparison to other structural forms for the same purpose, thin-walled tubes are attractive because they have lighter weight, greater flexibility, and improved torsion resistance. Their large diameter also gives them large moment of inertia with small cross-section areas, making them efficient elements for wind-induced bending moments. Although most current designs, which do not push the limits of slenderness, are often governed by cyclic fatigue effects, the push for higher and thinner towers makes them more susceptible to deformation under large external loads, especially compression, that may cause them to fail in shell buckling. The buckling behavior of thin-walled tubes bearing larger external loads is strongly influenced by the tube's geometry, material properties, and wall thickness. Consequently, design and analysis procedures

need to be established that account for realistic tube geometry (including imperfections) and their interaction with a wide range of buckling modes.

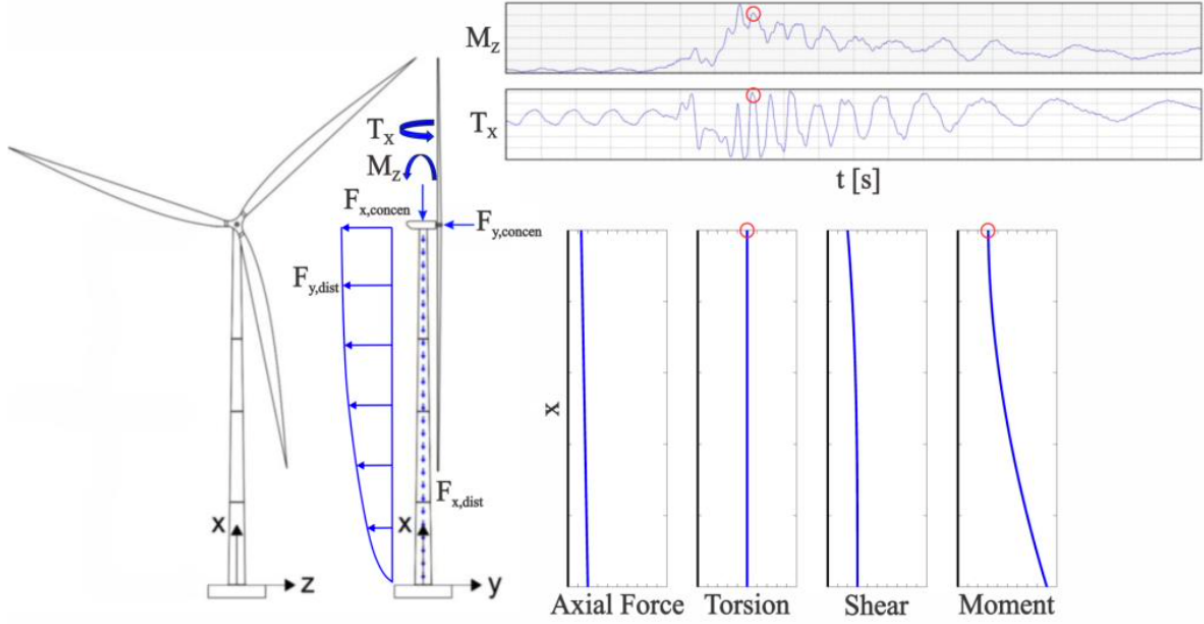


Figure 1: Illustration of the time-varying stochastic loading on a typical wind-turbine tower showing time histories of the moment  $M_z$  and torsion  $T_x$  at the tower top during operational conditions along with instantaneous distributions of axial force, torsion, shear, and moment in the tower. Image from (Ding et al. 2021)

### 1.2 Buckling of thin-walled structural tubes

In a typical finite element implementation, e.g. in our thin-walled tube of interest, buckling modes can be determined by solving the following eigenvalue problem:

$$(\mathbf{K}_E - \Lambda \mathbf{K}_G) \Phi = 0 \quad (1)$$

where  $\mathbf{K}_E$  is the elastic stiffness matrix of the initially perfect structure,  $\mathbf{K}_G$  is the geometric stiffness matrix,  $\Lambda = \text{diag}(\lambda_1, \lambda_2, \dots, \lambda_N)$  is a diagonal matrix of eigenvalues associated each eigenmode in  $\Phi = [\phi_1, \phi_2, \dots, \phi_N]$ . However, as previously mentioned, thin-walled turbine tower structural tubes are subjected to a complex combination of external forces. This becomes important because  $\mathbf{K}_G$  is dependent on the internal stress state in the structure. As a result, Eq. 1 will take different form in practice when the structure is subject to a pure axial compressive force  $P$ , i.e.,

$$(\mathbf{K}_E - \Lambda_P \mathbf{K}_G(P)) \Phi_P = 0 \quad (2)$$

than it will under a pure bending moment  $M$ , i.e.,

$$(\mathbf{K}_E - \Lambda_M \mathbf{K}_G(M)) \Phi_M = 0 \quad (3)$$

or some combination of e.g., axial force  $P$ , bending moment  $M$ , shear force  $V$ , and torsion  $T$ , i.e.,

$$(\mathbf{K}_E - \Lambda_C \mathbf{K}_G(P, M, V, T)) \Phi_C = 0 \quad (4)$$

where  $\Phi_P, \Phi_M, \Phi_C$  are the buckling modes associated with pure compression, pure bending, and combined loading and  $\Lambda_P, \Lambda_M, \Lambda_C$  are the corresponding eigenvalues.

The buckling loads themselves are not of primary interest since observed strength in shells is often significantly below these values. However, the buckling modes are important for their role in understanding strength imperfection sensitivity (Koiter 1945). The question of which buckling modes are most important and influential for the stability of the structure over its lifetime is complicated by the existence of actual geometric imperfections, the shape of which may make certain buckling modes preferential while counteracting others.

### 1.3 GMNIA collapse simulation

A GMNIA collapse simulation, which may provide a reliable estimate of strength, provides an incremental solution to the following equilibrium problem:

$$\mathbf{F} = (\mathbf{K}_E(\mathbf{I}) - \mathbf{K}_G(P, M, V, T) - \mathbf{K}_M)\mathbf{d} = 0 \quad (5)$$

where  $\mathbf{K}_E(\mathbf{I})$  is the elastic stiffness matrix formed on the imperfect initial geometry (and typically updated during the incremental analysis),  $\mathbf{K}_G$  is the geometric stiffness matrix and is a function of the internal stress state developed from the external load  $\mathbf{F}(P, M, V, T)$ , in a given increment, and  $\mathbf{K}_M$  is a material reduction matrix to account for yielding which itself is a function of initial material imperfections and its implementation may often be embedded into a tangent stiffness  $\mathbf{K}$  as opposed to a separate reduction matrix, and  $\mathbf{d}$  is the deformations. Determination of  $\mathbf{I}$  for use in forming  $\mathbf{K}_E$  in the GMNIA analysis is of primary interest.

### 1.4 Goals of this study

Although many studies have been conducted to investigate the buckling strength of thin-walled tubes with geometric defects, they are often limited to specific dominant buckling modes. For example, it is common to approximate imperfections ( $\mathbf{I}$ ) by imposing geometric imperfections in the form of the first three buckling modes corresponding to a specified loading condition ( $\mathbf{I} = \sum_{i=1}^3 c_i \phi_{Pi}$ ). In the interest of deriving a more general means of modeling imperfections we conduct a comprehensive study on the buckling strength sensitivity to the interaction of complex, higher-mode imperfections in thin-walled tubes, aiming to elucidate trends that can inform a novel stochastic expansion derived herein, and ultimately improving the practice of tube design and analysis.

We specifically explore geometric imperfections defined by combinations of the first one hundred axial and bending buckling modes with different magnitudes and analyze the resulting imperfect tubes through GMNIA under an externally applied bending moment. We then observe trends in the sensitivity of the buckling strength to imperfections imposed as combinations of two modes (either axial or bending modes). We further organize the mode shapes based on a characteristic length-scale (referred to as a buckling mode wavelength) to observe trends in the modal combinations with the greatest impact on buckling strength. We present the results of these analyses along with some observations in Section 4.

## 2. Modeling geometric imperfections

### 2.1 *Prior studies*

Imperfection models generally take one of four approaches: (1) worst, (2) stimulating, (3) realistic (categories per Wintersetetter and Schmidt 2002) or (4) stochastic (Elishakoff, 2000). See Castro et al. (2014) for a comprehensive summary and analysis of the sensitivity of tubes to imperfections. These four categories should not be considered mutually exclusive.

The concept of a worst imperfection is attractive from a deterministic standpoint but problematic as it is detached from expected actual imperfections. Koiter (1945) convincingly derived an argument for the lowest buckling modes to provide the worst imperfections, at least in the elastic case, but countless studies (see e.g., Castro et al. (2014)) have not borne this out for full GMNIA collapse simulations of steel shells. Nonetheless, the concept of worst imperfection lives on even in the latest Eurocode for shell structures (Eurocode 3 Part 1-6, 2021).

The notion of a stimulating imperfection is grounded in the observation that the strength difference between including any imperfection and no imperfection is often quite large – therefore, the shape is not as important as the inclusion of some imperfection. This is an attractive concept for its simplicity, and the buckling modes are a clear choice for such imperfections. However, in wind turbine support towers a major source of imperfection is the distortion that results from welding the cans together to form the tube (Rotter and Teng 1989, Sadowski et al. 2015). The resulting “weld depression” imperfection has been shown to be an excellent “stimulating” imperfection, with large strength sensitivity, even if it is not always well correlated with observed collapse mechanisms (Mahmoud et al. 2016, Sadowski et al. 2015).

The attractiveness of using realistic imperfections is clear – as the model is closer to reality; however numerous challenges exist. Of course, modelers interpret realistic imperfections in different ways – e.g., capturing the weld depression might be considered realistic vs. just using the first buckling mode. In general, realistic implies: “based on direct measurement” in some sense. Gathering the imperfection data on large tubes is complex and time consuming (Singer et al. 2002, Sadowski et al. 2022), even with the advent of new laser scanning and other technologies (Mirzaie et al. 2018, 2020). In design, engineers don’t have data on the actual tube they are designing, so “realistic” must be in a probabilistic sense.

Any field, such as imperfections, can be considered in a stochastic manner so numerous approaches have been applied to shell geometric imperfections with Elishakoff (2000) providing an excellent summary and Wang et al. (2022) providing a very recent example. Here we seek a new stochastic expansion that can be utilized to achieve our aims of realistic, stimulating imperfections.

### 2.2 *Hybrid stochastic expansion*

A relatively broad set of geometric imperfections can be sympathetic with the buckling modes of a thin-walled tube structure. This is demonstrated by so-called cross-section signature curves (Ding et. al. 2021), which show that for any specified tube length a very large number of buckling mode shapes yield similar buckling loads. It is therefore critical to understand which of these buckling modes will practically arise in real, observable geometric imperfections and which will not. Of

course, the magnitude and precise shape of defects are usually unknown in practical applications and can vary significantly (and stochastically) from one tube to another. These two factors therefore call for geometric imperfections to be expressed in a stochastic expansion of the following form:

$$I(\mathbf{x}) = \sum_{i=1}^{\infty} C_i \phi_i(\mathbf{x}) \quad (6)$$

where  $\phi_i(\mathbf{x})$  are orthogonal basis functions and  $C_i$  are random variables. Many possible expansions of this form are possible, with each form using a different set of basis functions. For example, the commonly used Spectral Representation Method (Papadopoulos and Papadrakakis, 2005; Zeinoddini and Schafer, 2012) employs a Fourier basis while the Karhunen-Loeve expansion (Craig and Roux, 2008) defines the basis functions as the eigenfunctions of the covariance. For cylinder buckling problems, it makes sense to employ a physically relevant basis associated with the Eigen buckling modes of the structure. This approach has been employed by several researchers in previous studies (Sadowski, 2022; Ismail et. al. 2019).

However, the discussion above implies that the construction of this expansion in Eq. 6 is not straightforward. The complication arises from two fundamental issues: (i) The buckling modes are loading dependent; (ii) The expansion in Eq. 6 must be truncated to include only  $n$  terms and, for practical reasons,  $n$  must be small. Let us first address issue (i). Because the buckling modes depend on the loading conditions, it is not obvious which set of buckling modes are optimal for such an expansion. Should the expansion be expressed in terms of axial modes, bending modes, or modes from some combined loading conditions? Given that the structure will see a wide range of loading conditions in its lifetime, the answer is not clear.

The second issue arises because of both the preponderance of buckling modes that result in comparable strengths and the fact that there are no guarantees on the compactness of the expansion necessary to reproduce real imperfections using a basis derived from buckling modes. This contrasts with methods like the Karhunen-Loeve expansion, for example, which is mean-square optimal in its representation of the covariance function. We therefore seek an expansion constructed from an arbitrary set of buckling modes (e.g., bending and/or axial modes) that includes a compact set of modes that will have both a strong influence on the strength of the structure and a significant contribution to realistic imperfection shapes. For this, we propose the following expansion.

Consider that an arbitrary stochastic imperfection shape can be expanded equivalently in terms of the bending buckling modes  $\phi_M$  or the axial buckling modes  $\phi_P$  as:

$$I(\mathbf{x}) = \sum_{i=1}^{\infty} \alpha_i \phi_{Mi}(\mathbf{x}) = \sum_{j=1}^{\infty} \beta_j \phi_{Pj}(\mathbf{x}) \quad (7)$$

Ideally, we seek a representation that expands in terms of both  $\phi_M$  and  $\phi_P$  and allows us to choose the modes that are most important. But we recognize that, in general the bending modes and axial modes are not orthogonal to one another (i.e.,  $\langle \phi_{Mi}, \phi_{Pj} \rangle \neq 0$ ) and this expansion therefore does not have a valid basis. In fact, because the bending modes and the axial modes both provide a complete basis, we see that any axial mode (for example,  $\phi_{Pj}$ ) can be expanded as a series of bending modes as follows:

$$\phi_{Pj}(\mathbf{x}) = \sum_{k=1}^{\infty} \gamma_{jk} \phi_{Mk}(\mathbf{x}) \quad (8)$$

Using Eq. 8, we can therefore express the imperfections through a hybrid expansion of the following form

$$I(\mathbf{x}) = \sum_{i=1}^{\infty} \alpha_i \phi_{Mi}(\mathbf{x}) + \sum_{j=1}^{\infty} \beta_j (\phi_{Pj}(\mathbf{x}) - \sum_{k=1}^{\infty} \gamma_{jk} \phi_{Mk}(\mathbf{x})) \quad (9)$$

by recognizing that  $\phi_{Pj}(\mathbf{x}) - \sum_{k=1}^{\infty} \gamma_{jk} \phi_{Mk}(\mathbf{x}) = 0$ . Expanding Eq. 9 yields:

$$I(\mathbf{x}) = \sum_{j=1}^{\infty} \beta_j \phi_{Pj}(\mathbf{x}) + \sum_{i=1}^{\infty} \alpha_i \phi_{Mi}(\mathbf{x}) - \sum_{j=1}^{\infty} \sum_{k=1}^{\infty} \beta_j \gamma_{jk} \phi_{Mk}(\mathbf{x}) \quad (10)$$

where the first two terms represent the (redundant) expansion in terms of both axial and bending modes and the final term represents the projections of the axial modes onto the basis of bending modes. Through simple rearrangement of the terms in Eq. 10 we can express the imperfection through a general *hybrid* expansion in terms of both  $\phi_M$  and  $\phi_P$  by:

$$I(\mathbf{x}) = \sum_{j=1}^{\infty} \beta_j \phi_{Pj}(\mathbf{x}) + \sum_{i=1}^{\infty} (\alpha_i - \sum_{j=1}^{\infty} \beta_j \gamma_{ji}) \phi_{Mi}(\mathbf{x}) \quad (11)$$

To make this expansion practical, we need to truncate it to include only a finite number of terms. Let us begin by truncating the set of axial modes to include  $N_P$  terms. This can be expressed as:

$$I(\mathbf{x}) = \sum_{j=1}^{N_P} \beta_j \phi_{Pj}(\mathbf{x}) + \sum_{i=1}^{\infty} (\alpha_i - \sum_{j=1}^{N_P} \beta_j \gamma_{ji}) \phi_{Mi}(\mathbf{x}) \quad (12)$$

Next, we wish to truncate the basis of bending modes to  $N_M$  terms. However, doing so will also remove the projection of the axial modes onto the higher-order modes ( $N > N_M$ ). We, therefore, split the second term of Eq. 12, resulting in the following expansion:

$$I = \sum_{j=1}^{N_P} \beta_j \phi_{Pj} + \sum_{i=1}^{N_M} (\alpha_i - \sum_{j=1}^{N_P} \beta_j \gamma_{ji}) \phi_{Mi} + \sum_{i=N_M+1}^{\infty} (\alpha_i - \sum_{j=1}^{N_P} \beta_j \gamma_{ji}) \phi_{Mi} \quad (13)$$

where the  $x$  dependence has been removed for brevity. The truncated expansion in Eq. 13 is composed of three terms:

1.  $N_P$  axial buckling modes (first term)
2.  $N_M$  bending buckling modes (second term)
3. A residual (third term)

This expansion now allows us to select an arbitrary set of axial and bending modes and build an expansion of the imperfection in terms of this set. The residual arises from the components of the axial modes projected onto the bending mode basis that cannot be removed because the buckling mode basis is truncated. In other words, the expansion of axial buckling mode  $\phi_{Pj}, j \leq N_P$  will have terms associated with higher order bending modes  $\phi_{Mi}, i > N_M$  that we cannot remove because the basis set is truncated at  $N_M$ . In practice, the expansion will be assembled only from the first two terms of Eq. 13 but recognizing that the residual can be quantified (and ideally minimized).

Finally, we note that expansion in Eq. 13 can easily be modified to consider first the bending moments and removing the bending mode projection on the axial mode basis by simply switching the bending and axial modes in the expansion. We further note that, through a similar analysis, more complex expansions that account for additional modes (e.g., torsion modes) can be derived.

### 3. Methodology and model setup

In light of the previous discussion and the proposed hybrid stochastic expansion, we conducted a study to investigate the sensitivity of thin-walled cylindrical shell structures to combinations of axial and bending buckling modes. First, the eigenvalue buckling analysis of the perfect tube structure is performed (Section 1.2) to generate the first one hundred buckling modes under pure bending and pure axial loading, respectively. Combinations of the extracted mode shapes were then imposed as imperfections with two different magnitudes for geometric material nonlinear imperfection analysis (GMNIA) (Section 1.3) under bending moment to observe the change in tube strength, thus indicating the sensitivity of the tube section to various combined mode imperfection.

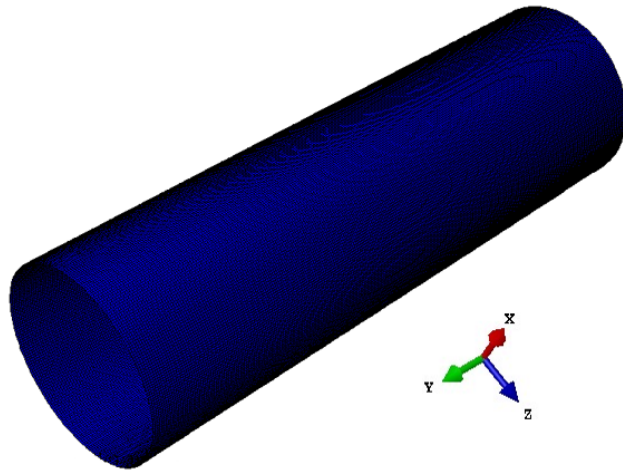


Figure 2: Geometry of the structure examined in this study

Simulations in this study were conducted using ABAQUS 2020. The model shown in Fig. 2, and whose first one hundred axial modes are illustrated in Fig. 3 and first one hundred bending modes are illustrated in Fig. 4, comprised a thin-walled tube of radius 501.65 mm, length 3302 mm, and thickness 4.7625 mm, using 776,127 four-node S4 shell elements to provide sufficient discretization to capture the bending buckling response of the tube. Both ends of the tube are fixed except for rotation in the X and Z directions. The tube material is modeled to represent S355 steel using the true stress-strain material model in DNV-RP-C208 (2013) with elastic modulus equal to 210,000 MPa, Poisson's ratio of 0.3, yield stress of 357 MPa and ultimate stress of 541.6 MPa. Simulations were performed with the Riks method (Riks et. al. 1979). In our case, the bending moment is applied at both ends of the tube about the X-direction and increases at a constant rate until the structure buckles.

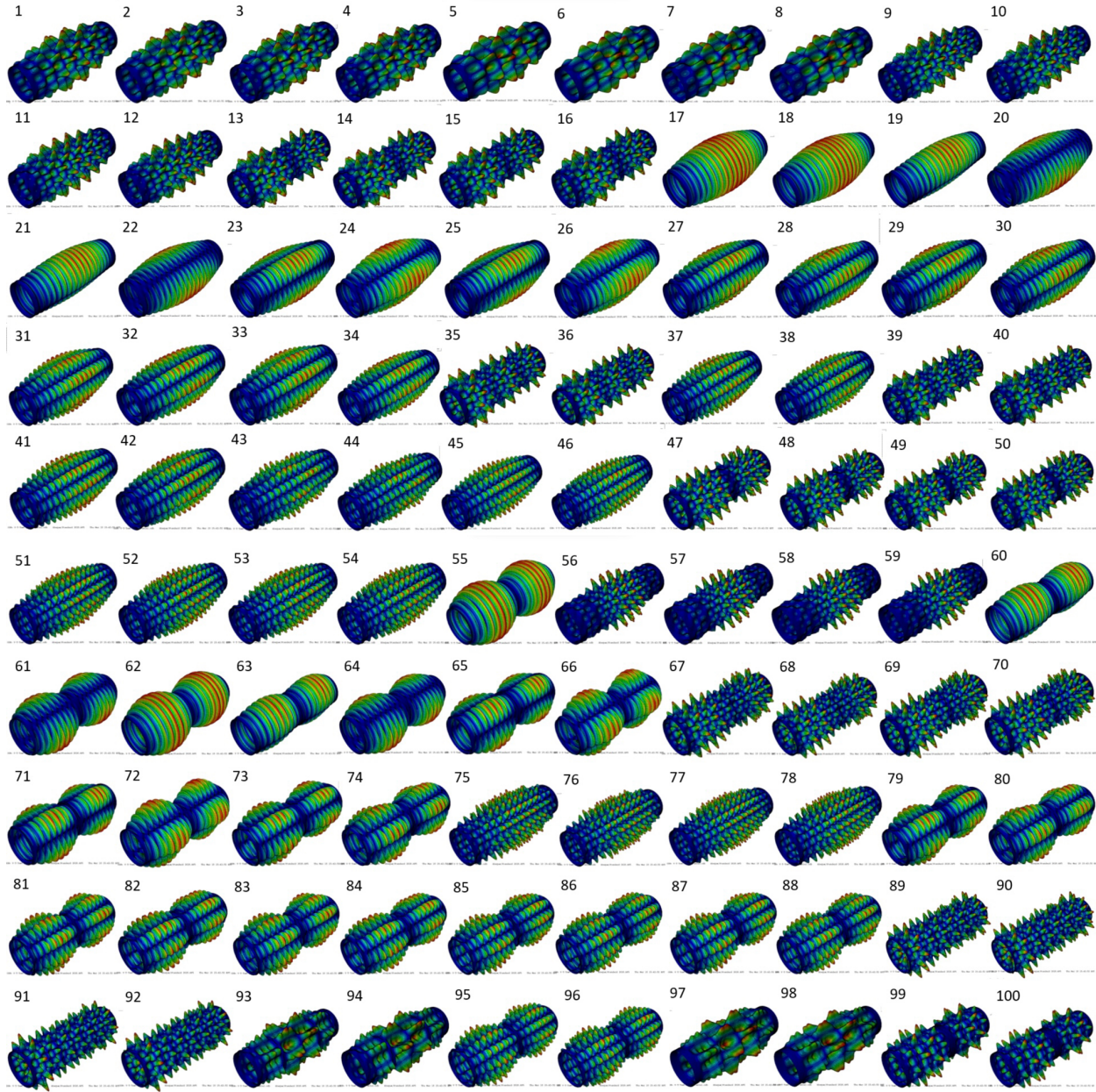


Figure 3: First 100 axial mode shapes.

The imposed imperfection magnitudes are taken from those specified in Eurocode EN 1993-1-6:2007 as:

$$m = 4u\sqrt{tr} \quad (13)$$

where  $m$  is the magnitude,  $t$  represents the thickness of the tube,  $r$  is the tube radius, and  $u$  is a specific parameter related to the design classes (Class A and C) defined in EN 1993-1-6:2007. For class A,  $u$  is set to be 0.006, and for Class C,  $u$  is set to be 0.016. The imperfection magnitude  $m$  is then multiplied by the normalized buckling mode deflection from linear buckling analysis and the resulting imperfection is imposed on the pristine model. For combinations of modes, the modal displacements are added and then normalized. The normalized combined mode displacements are

then multiplied by the magnitude  $m$  and imposed on the pristine model to create an imperfect geometry. This process was repeated for all  $100 \times 100$  combinations of two axial buckling modes and  $100 \times 100$  combinations of two bending buckling modes under both class A and class C magnitude imperfections, for a total of 40,000 GMNIA simulations. From each simulation, the moment capacity under imperfection class A,  $M_A$ , and under imperfection class C,  $M_C$ , was recorded.

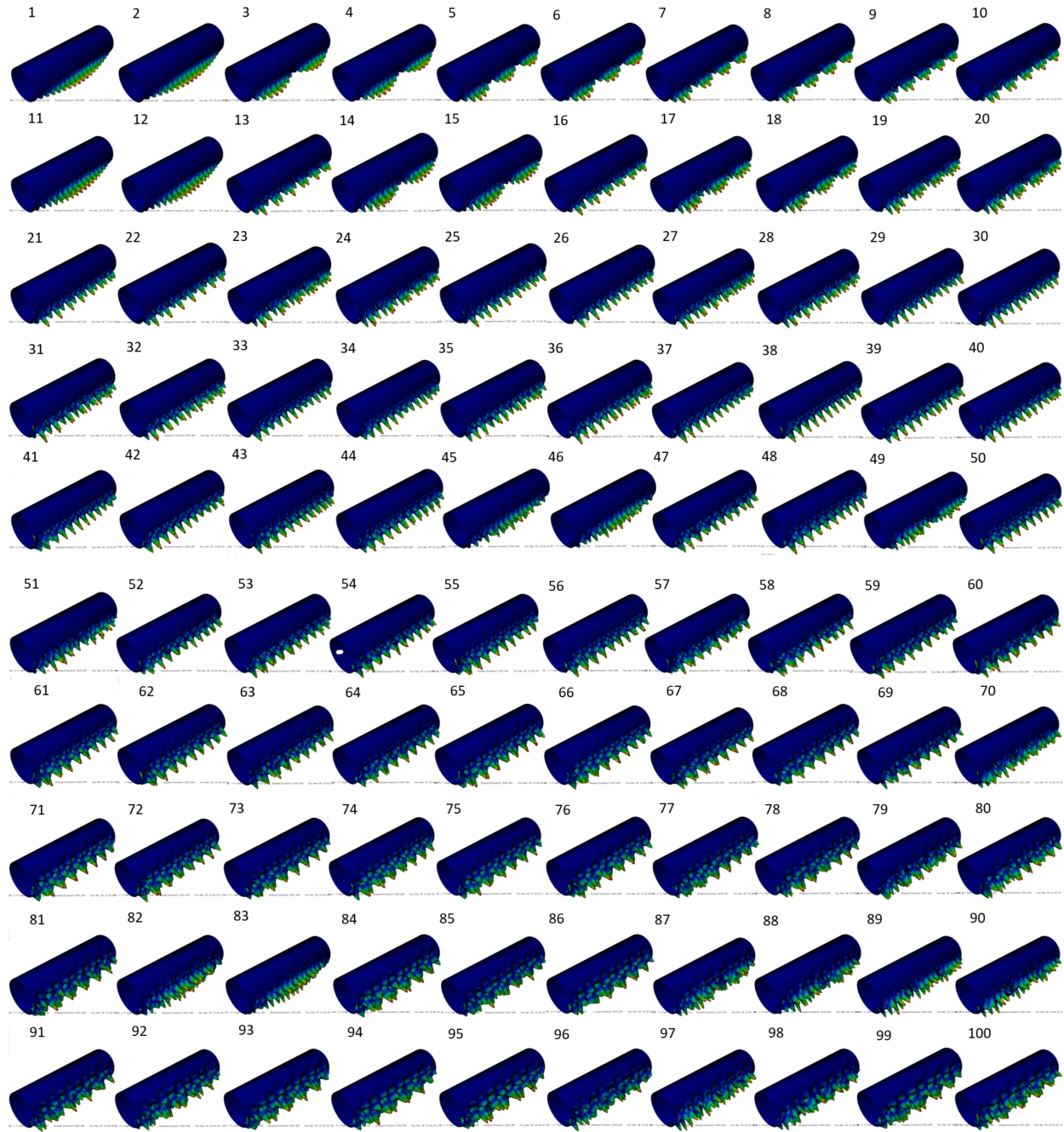


Figure 4: First 100 bending mode shapes.

#### 4. Results

Strength sensitivity for each combination of mode imperfections was measured by computing the relative loss of moment resistance capacity from increasing imperfection magnitude from class A to class C as  $\frac{M_A - M_C}{M_A}$ . We then plot these bending strength sensitivity values for each combination of imperfections using a heat map in Fig. 5. Here we see that certain modes, e.g., modes 24, 26, 66 and 72, have significant influence on the strength of the cylinder when they are paired with nearly any other mode. This is clearly indicated by the red stripes that can be observed for these mode numbers. Moreover, we can see distinct regions where interactions seem to be particularly impactful. For example, in the upper-right quadrant, modes 78 – 88 seem to interact quite strongly with modes 17 – 34.

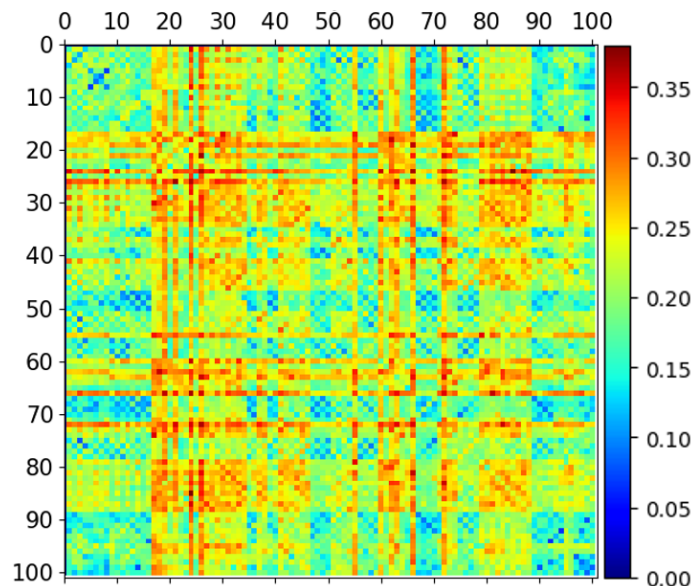


Figure 5: Bending strength sensitivity  $(M_A - M_C) / M_A$  for models with imperfections introduced by combined axial buckle modes, organized by mode order.

To gain additional insight into the physical mechanisms at play in these sensitivities, we compute two characteristic length-scales for each mode shape, which we refer to as the longitudinal and circumferential wavelengths. These wavelengths are computed from the mode shape by identifying the extreme values (maximum positive and maximum negative values) and computing the average distance between the nearest extrema (of the same sign). This is an admittedly crude measure, but it serves as a first attempt to systematically assign a scalar metric to characterize the length-scale of buckling modes.

The reorganized colormaps are shown in Fig. 6. Fig. 6a shows the bending strength sensitivities re-organized by circumferential wavelength, while Fig. 6b shows the bending strength sensitivities re-organized by longitudinal wavelength. Here we observe some interesting trends. When the modes are reorganized by circumferential wavelength, those cases where both modes have small wavelength (i.e., having many circumferential waves in the buckling mode) are relatively insensitive to imperfections. Meanwhile, when both modes have large wavelengths (i.e., having a small number of circumferential waves) the sensitivity is high. That is, increasing the magnitude of pairs of imperfections with large wavelength from class A to class C can decrease the strength of the cylinder by 30% or more. We see from Fig. 6b that the opposite trend is true when the modes

are reorganized according to their longitudinal wavelength. The strength sensitivity is large for modes with short longitudinal wavelength and small for modes with long wavelength. This means that the strength is highly sensitive to modes that combine many longitudinal waves with few circumferential waves.

Finally, we note that the method used for automated estimation of the mode wavelength is simplistic and may not be robust in all cases. There are likely several cases where the automated procedure yields an inaccurate estimate of the wavelength. This likely contributes to the lack of smoothness in these plots. We are currently exploring more robust means of estimating a characteristic length-scale for the mode shapes.

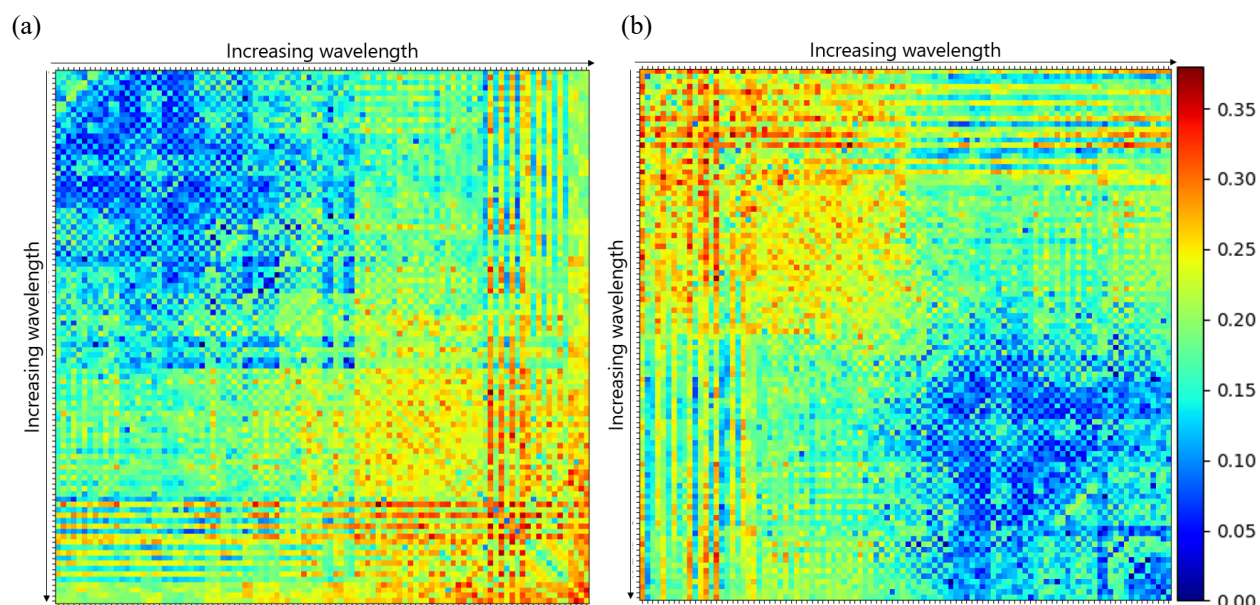


Figure 6: Bending strength sensitivity  $(M_A - M_C)/M_A$  for axial imperfection combinations organized by (a) the circumferential wavelengths of the axial modes; (b) the longitudinal wavelengths of the axial modes.

The same analysis was repeated for models with combinations of bending mode imperfections of class A and class C magnitude. Again, an external bending moment is then applied to these imperfect models until buckling is observed. Fig. 7 shows the colormap of strength sensitivity  $\frac{M_A - M_C}{M_A}$  for each model with imperfections as combinations of the first one hundred bending buckling modes, where the plots are organized by mode number. Unlike the case where we imposed axial mode imperfections, we see a clear trend where the sensitivity generally increases with mode number. This seems to indicate that, while the lower mode numbers may likely to have lower strength when the modal imperfection is first introduced (i.e., for class A magnitude), they are less sensitive to an increase in the magnitude than the higher modes. Moreover, these results differ from the axial mode imperfections in that there do not appear to be single modes that show uniformly high sensitivity. Where the colormaps for the axial imperfections showed certain “stripes” that indicated certain mode numbers exhibit high sensitivity regardless of which other modes they are combined with, these same features are not observed when bending mode imperfections are imposed.

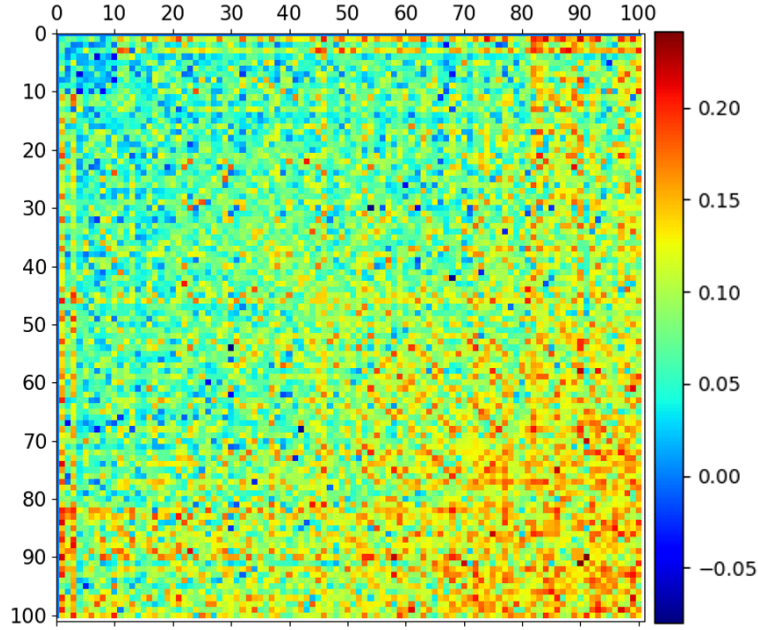


Figure 7: Bending strength sensitivity  $(M_A - M_C) / M_A$  for models with imperfections introduced by combined bending buckling modes, organized by mode order.

Once again, we also organized the heatmap to show the bending buckling sensitivity for mode combinations organized by longitudinal and circumferential wavelength. This time we do not see any meaningful trend. The buckling strength sensitivity does not seem to change systematically with the wavelength of the buckling modes, but rather it seems to be more strongly influenced by the mode number.

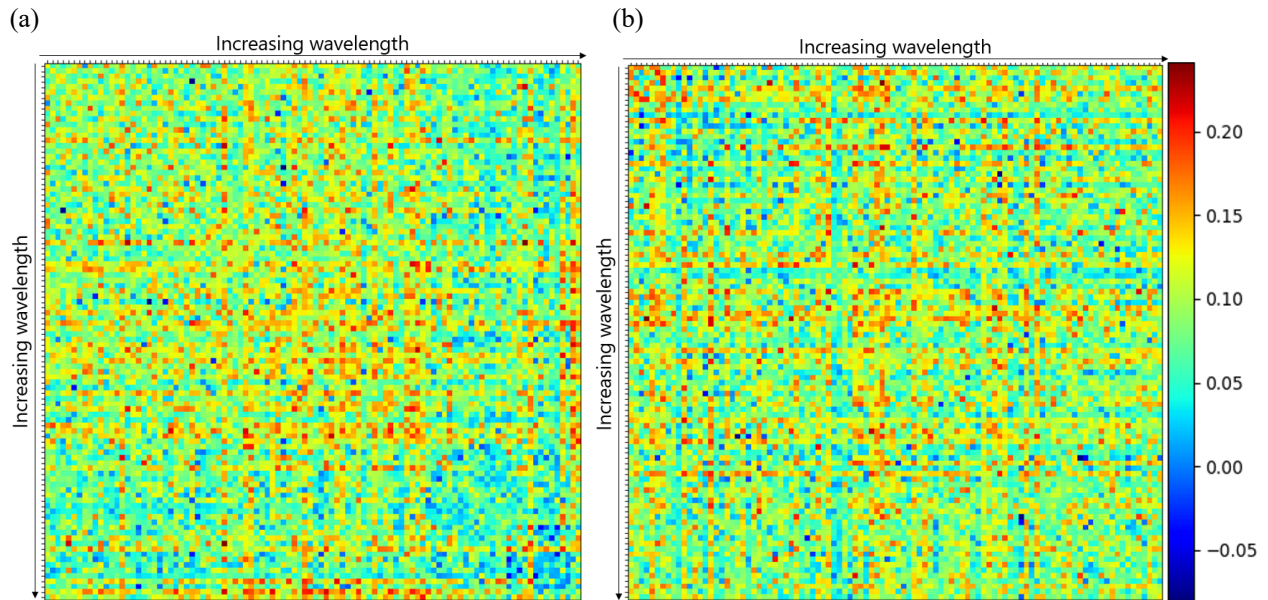


Figure 8: Bending strength sensitivity  $(M_A - M_C) / M_A$  for bending mode imperfection combinations organized by (a) the circumferential wavelengths of the bending modes; (b) the longitudinal wavelengths of the bending modes.

Finally, we highlight that the diagonal terms in each of the plots correspond to the superposition of a single mode with itself – or, in effect, a doubling of the imperfection magnitude for a single

mode. Interestingly, for both cases where axial modes and bending modes are imposed as imperfections, we observe that coupling two different modes can cause a larger strength decrease than simply doubling the magnitude of a single mode imperfection. That is, quite often the off-diagonal terms of the sensitivity matrix are substantially larger than the diagonal terms. This means that imperfections imposed based on a single mode may not be conservative because, in fact, adding a second mode of imperfection may serve to reduce the strength more than simply increasing the magnitude of the single mode imperfection.

## 5. Conclusion

This study has presented an investigation of the buckling strength sensitivity for slender cylindrical tube structures subjected to bending with geometric imperfections defined through combinations of axial and bending buckling modes. The study is motivated by the need to establish new models to represent geometric imperfections that are both informed by the buckling mechanics and can be derived from observed imperfection data. A new expansion method was proposed that considers geometric imperfections to be expressed in terms of combinations of buckling modes under different loading conditions. We specifically derive the expansion for combined axial and bending buckling modes. This expansion begs the question of which modes (bending and axial) should be included when constructing the model. To address this question, it's therefore important to evaluate the sensitivity of the structure to various combinations of mode shaped imperfections; the results of which can be used to assess which terms are the most mechanically important in the expansion.

We specifically considered the first one hundred axial buckling modes and the first one hundred bending buckling modes for a specified thin-walled tube structure as determined through a linear Eigen buckling analysis. We then imposed geometric imperfections as combinations of pairs of these modes having Eurocode Class A and Class C magnitude imperfections and solved for the buckling strength under pure bending using GMNIA in ABAQUS. This comprised a set of 40,000 simulations from which we drew the following conclusions about the interaction of mode shaped imperfections on the buckling strength. 1. Imperfections in the form of multiple interacting modes can reduce the strength substantially more than simply increasing the magnitude of a single mode imperfection proportionally. 2. The buckling strength sensitivity under bending with axial mode imperfections shows a clear dependence on the length-scale of the axial modes imposed, with modes having smaller longitudinal wavelengths and longer circumferential wavelengths being more influential. 3. The buckling strength sensitivity under bending with bending mode imperfections shows a clear dependence on mode number but does not show dependence on the buckling mode length-scale.

## Acknowledgment

The authors gratefully acknowledge the support of the National Science Foundation under Grant No. 1912481. Any opinions, findings, and conclusions or recommendations expressed in this material are those of the authors and do not necessarily reflect the views of the National Science Foundation.

## References

AISC (American Institute of Steel Construction). (2020). "Specification for Structural Steel Buildings." Chicago, IL: AISC.

- Bonada, J., Casafont, M., Roure, F., & Pastor, M. M. (2012). "Selection of the initial geometrical imperfection in nonlinear FE analysis of cold-formed steel rack columns." *Thin-walled structures*, 51, 99-111.
- Calladine, C. R. (1995). "Understanding imperfection-sensitivity in the buckling of thin-walled shells." *Thin-Walled Structures*, 23(1-4), 215-235.
- Castro, S. G., Zimmermann, R., Arbelo, M. A., Khakimova, R., Hilburger, M. W., & Degenhardt, R. (2014). "Geometric imperfections and lower-bound methods used to calculate knock-down factors for axially compressed composite cylindrical shells." *Thin-Walled Structures*, 74, 118-132.
- Craig, K. J., & Roux, W. J. (2008). "On the investigation of shell buckling due to random geometrical imperfections implemented using Karhunen–Loeve expansions." *International Journal for Numerical Methods in Engineering*, 73(12), 1715-1726.
- Ding, V., Abdelrahman, A.H.A., Lin, D., Shields, M.D., Myers, A.T., Krabbe, M., & Schafer, B.W. (2021). "Classical and finite element methods for elastic buckling of cylindrical shells." In *Proceedings of the Annual Stability Conference Structural Stability Research Council/NASCC: The Steel Conference*, Louisville, KY.
- DNV-RP-C208. (2013). "Determination of structural capacity by non-linear finite element analysis methods."
- Elishakoff, I. (2000). "Uncertain buckling: Its past, present and future." *International Journal of Solids and Structures*, 37(46), 6869-6889.
- EN 1993-1-6:2007. (2007). "Eurocode 3: Design of steel structures - Part 1-6: Strength and stability of shell structures"
- Farzarian, S., Louhghalam, A., Schafer, B. W., & Tootkaboni, M. (2018). "Geometric imperfections in shell finite element models of CFS members-A review of current state of practice." In *Proceedings of the Annual Stability Conference Structural Stability Research Council/NASCC: The Steel Conference*, Baltimore, MD.
- Friedrich, L., Schmid-Fuertes, T. A., & Schröder, K. U. (2015). "Comparison of theoretical approaches to account for geometrical imperfections of unstiffened isotropic thin walled cylindrical shell structures under axial compression." *Thin-Walled Structures*, 92, 1-9.
- Ismail, M. S., Ifayefunmi, O., & Fadzullah, S. H. S. M. (2019). "Buckling of imperfect cylinder-cone-cylinder transition under axial compression." *Thin-Walled Structures*, 144, 106250.
- Koiter, W.T. (1945). "The Stability of Elastic Equilibrium." *Ph.D. Dissertation TU-Delt*.
- Lynch, C., Murphy, A., Price, M., & Gibson, A. (2004). "The computational post buckling analysis of fuselage stiffened panels loaded in compression." *Thin-walled structures*, 42(10), 1445-1464.
- Mahmoud, A., Torabian, S., Jay, A., Mirzaie, F., Myers, A. T., Smith, E., & Schafer, B. W. (2016). "Collapse Analyses on Spirally Welded Tapered Tubes using EC3 Generated Imperfections." In *Proceedings of the Annual Stability Conference Structural Stability Research Council/NASCC: The Steel Conference*, Orlando, FL.
- Mirzaie, F., Myers, A. T., Jay, A., Mahmoud, A., Torabian, S., Smith, E., Schafer, B. W. (2018). "Imperfection measurements to predict buckling behavior of slender steel tubes." *Thin-Walled Structures*, 123, 270-281.
- Mirzaie, F., Myers, A. T., Jay, A., Mahmoud, A., Smith, E., Schafer, B. W. (2020). "Analysis of geometric imperfections of spirally welded slender steel tubes." *Thin-Walled Structures*, 146
- Papadopoulos, V., & Papadrakakis, M. (2005). "The effect of material and thickness variability on the buckling load of shells with random initial imperfections." *Computer Methods in Applied Mechanics and Engineering*, 194(12-16), 1405-1426.
- Pastor, M. M., Casafont, M., Bonada, J., & Roure, F. (2014). "Imperfection amplitudes for nonlinear analysis of open thin-walled steel cross-sections used in rack column uprights." *Thin-walled structures*, 76, 28-41.
- Paulo, R. M. F., Teixeira-Dias, F., & Valente, R. A. F. (2013). "Numerical simulation of aluminium stiffened panels subjected to axial compression: Sensitivity analyses to initial geometrical imperfections and material properties." *Thin-Walled Structures*, 62, 65-74.
- Riks, E. (1979). "An incremental approach to the solution of snapping and buckling problems." *International journal of solids and structures*, 15(7), 529-551.
- Rotter, J. M., & Teng, J. G. (1989). "Elastic stability of cylindrical shells with weld depressions." *Journal of Structural Engineering*, 115(5), 1244-1263.
- Sadovský, Z., & Kriváček, J. (2020). "Influential geometric imperfections in buckling of axially compressed cylindrical shells—A novel approach." *Engineering Structures*, 223, 111170.
- Sadowski, A. J., Van Es, S. H., Reinke, T., Rotter, J. M., Gresnigt, A. N., & Ummenhofer, T. (2015). "Harmonic analysis of measured initial geometric imperfections in large spiral welded carbon steel tubes." *Engineering Structures*, 85, 234-248.
- Sadowski, A.J.; Seidel, M., and Schafer, B.W. (2022). "Recommendations for surface imperfections surveys for thin-walled metal wind turbine support towers." *Proceedings of the ASME 2022 International Offshore Wind Tunnel Conference IOWTC2022*, Bostom, MA.

- Sadowski, A. J. (2022). "Automated classification of linear bifurcation buckling eigenmodes in thin-walled cylindrical shell structures." *Advances in Engineering Software*, 173, 103257.
- Schafer, B. W., Li, Z., & Moen, C. D. (2010). "Computational modeling of cold-formed steel." *Thin-walled structures*, 48(10-11), 752-762.
- Weingarten, V. I., Seide, P., & Peterson, J. P. (1968). "Buckling of thin-walled circular cylinders" NASA-SP-8007.
- Singer, J., Arbocz, J., & Weller, T. (2002). "Buckling experiments: experimental methods in buckling of thin-walled structures, volume 2: shells, built-up structures, composites and additional topics (Vol. 2)." John Wiley & Sons.
- Wang, H., Guillemot, J., Schafer, B. W., & Tootkaboni, M. (2022). "Stochastic analysis of geometrically imperfect thin cylindrical shells using topology-aware uncertainty models." *Computer Methods in Applied Mechanics and Engineering*, 393.
- Winterstetter, T. A., & Schmidt, H. (2002). "Stability of circular cylindrical steel shells under combined loading." *Thin-Walled Structures*, 40(10), 893-909.
- Zeinoddini, V. M., & Schafer, B. W. (2012). "Simulation of geometric imperfections in cold-formed steel members using spectral representation approach." *Thin-Walled Structures*, 60, 105-117.
- Zhou, Z., Wu, J., & Meng, S. (2014). "Influence of member geometric imperfection on geometrically nonlinear buckling and seismic performance of suspen-dome structures." *International Journal of Structural Stability and Dynamics*, 14(03), 1350070.